International Journal of Fluid Machinery and Systems
Vol. 2, No. 2, January 2009

Original Paper

Prediction of Cavitation Intensity in Pumps Based on Propagation Analysis of Bubble Collapse Pressure Using Multi-Point Vibration Acceleration Method

Masashi Fukaya[1], Shigeyoshi Ono[2] and Ryujiro Udo[3]

[1]Mechanical Engineering Research Laboratory, Hitachi, Ltd.
832-2, Horiguchi, Hitachinaka, Ibaraki, 312-0034, Japan

[2]Engineering Cluster, Hitachi Technologies and Services, Ltd.
603, Kandatsu, Tsuchiura, Ibaraki, 300-0013, Japan

[3]Mechanical Engineering Research Laboratory, Hitachi, Ltd.
832-2, Horiguchi, Hitachinaka, Ibaraki, 312-0034, Japan
(Present Affiliation: Social Infrastructure & Industrial Machinery Systems Group,
Hitachi Plant Technologies, Ltd.
603, Kandatsu, Tsuchiura, Ibaraki, 300-0013, Japan)

Abstract

We developed a 'multi-point vibration acceleration method' for accurately predicting the cavitation intensity in pumps. Pressure wave generated by cavitation bubble collapse propagates and causes pump vibration. We measured vibration accelerations at several points on a casing, suction and discharge pipes of centrifugal and mixed-flow pumps. The measured vibration accelerations scattered because the pressure wave damped differently between the bubble collapse location and each sensor. In a conventional method, experimental constants are proposed without evaluating pressure propagation paths, then, the scattered vibration accelerations cause the inaccurate cavitation intensity. In our method, we formulated damping rate, transmittance of the pressure wave, and energy conversion from the pressure wave to the vibration along assumed pressure propagation paths. In the formulation, we theoretically defined a 'pressure propagation coefficient,' which is a correlation coefficient between the vibration acceleration and the bubble collapse pressure. With the pressure propagation coefficient, we can predict the cavitation intensity without experimental constants as proposed in a conventional method. The prediction accuracy of cavitation intensity is improved based on a statistical analysis of the multi-point vibration accelerations. The predicted cavitation intensity was verified with the plastic deformation rate of an aluminum sheet in the cavitation erosion area of the impeller blade. The cavitation intensities were proportional to the measured plastic deformation rates for three kinds of pumps. This suggests that our method is effective for estimating the cavitation intensity in pumps. We can make a cavitation intensity map by conducting this method and varying the flow rate and the net positive suction head (*NPSH*). The map is useful for avoiding the operating conditions having high risk of cavitation erosion.

Keywords: Cavitation intensity, Bubble collapse, Pressure propagation, Vibration acceleration, Pump

1. Introduction

Downsized pumps are required for reducing production costs. For some downsized pumps, cavitation erosion damages the impeller or the casing, and the prediction of cavitation erosion is important for maintaining pump reliability. Cavitation erosion caused by cavitation bubble collapse is closely correlated with cavitation intensity. Therefore, cavitation intensity estimation is a promising method for predicting cavitation erosion. In representative conventional methods, the cavitation intensity was experimentally estimated using a piezoelectric sensor or a vibration acceleration sensor. The prediction accuracy of cavitation intensity depends on the distance between the bubble collapse location and the sensor.

In a conventional method, cavitation intensity is predicted using a piezoelectric sensor attached close to the bubble collapse location (Konno [1], Soyama [2], Maekawa [3]). The cavitation intensity is estimated by analyzing the distribution of the bubble impact force and frequency. The prediction accuracy of the cavitation intensity is high because the bubble collapse pressure is

Received May 21 2009; revised June 3 2009; accepted for publication June 3 2009: Review conducted by Prof. Yulin Wu. (Paper number O09014)
Corresponding author: Masashi Fukaya, Ph. D., masashi.fukaya.kp@hitachi.com

directly measured close to the bubble collapse location inside the pump. However, the sensor tends to peel off, and keeping it waterproof is problematic. Devices are needed for obtaining the electrical signals of the sensor from the rotating impeller and the shaft. Therefore, this method has unpractical aspects.

The bubble collapse pressure propagates in water and solids, and causes the vibration of a pump casing, suction and discharge pipes. In the method proposed in the TSJ Guideline 2003 [4], the cavitation intensity is predicted using vibration acceleration measured at one point outside the pump, e.g., on the casing. In the present paper, this conventional method is called 'single-point vibration acceleration method.' Measurement is easy because a vibration acceleration sensor is attached on the outside of the pump. Meanwhile, the prediction accuracy of cavitation intensity is not necessarily high because the sensor is located away from the bubble collapse location. When the pressure wave generated by the cavitation bubble collapse propagates from the bubble collapse location to the sensor, the damping rate is different in water and other materials of a pump casing, suction and discharge pipes. However, in the single-point vibration acceleration method, experimental constants are proposed without evaluating pressure propagation paths. Therefore, the vibration accelerations measured at different points are scattered, and the scattered vibration accelerations cause the inaccurate prediction accuracy of cavitation intensity. The experimental constants are also unpractical because they are required for each pump having different type, structure, and material.

We attempted to improve the prediction accuracy of cavitation intensity based on vibration acceleration analysis keeping the advantage of ease of measurement. For avoiding the experimental constants as proposed in the conventional method, we theoretically defined a 'pressure propagation coefficient,' which is a correlation coefficient between the vibration acceleration and the bubble collapse pressure. The pressure propagation coefficient was obtained by calculating

(1) the damping rate of the bubble collapse pressure propagating from the bubble collapse location to the sensor,
(2) the transmittance at the surface between different materials, e.g., water and iron casting, and
(3) the conversion from the energy of the pressure wave to that of the vibration.

The cavitation intensity was estimated based on the analysis of the measured vibration accelerations considering the pressure propagation coefficient. The prediction accuracy of cavitation intensity can be improved based on a statistical analysis of the multi-point vibration accelerations.

The cavitation intensities were predicted under four operating conditions in two types of hydraulic test pumps. To examine the prediction accuracy of the cavitation intensity, we compared the predicted cavitation intensities using our method and using the single-point vibration acceleration method with the plastic deformation rate of an aluminum sheet, which was attached in the cavitation erosion area of the impeller blade (Fukaya [5], Udo [6]).

2. Experimental Method

2.1 Vibration Acceleration Measurement

Figure 1 shows the arrangement of the vibration acceleration sensors in a hydraulic test pump. Four sensors were attached on the flange of the suction pipe (No. 1), the pipe wall (Nos. 2 and 3), and the casing (No. 4). The sensor positions were selected considering the 'pressure propagation coefficient' explained in the term 3.2. The sensors were piezoelectric vibration acceleration sensors (Ono Sokki, NP2110 [7]). The data sampling frequency was 40 kHz and the resonance frequencies of the sensors were

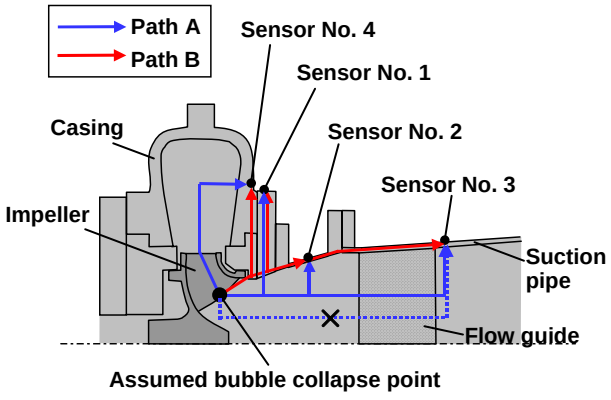

Fig. 1 Arrangement of vibration acceleration sensors and propagation path of collapse pressure in Cases 1 and 2 (Table 1)

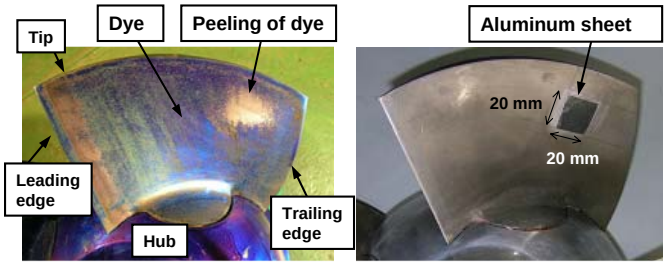

(a) Visualized cavitation erosion area (b) Aluminum sheet attached in cavitation erosion area

Fig. 2 Cavitation erosion area and aluminum sheet for measuring plastic deformation caused by bubble collapse in Case 4 (Table 1)

Table 1 Operating conditions of hydraulic test pumps

Case	Test pump	Peripheral velocity at impeller eye (Ue) [m/s]	Flow rate ($Q/Q_{\eta max}$) [-]
1	Centrifugal pump	17.2	60
2		20.1	60
3	Mixed-flow pump A	20.4	80
4	Mixed-flow pump B	22.5	85

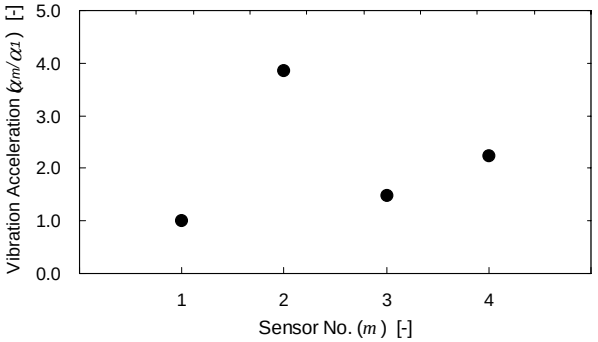

Fig. 3 Measured vibration accelerations in Case 1 (Table 1)

over 20 kHz. The data sampling frequency and the resonant frequencies were high enough because the vibration acceleration of below 10 kHz was required in our method. The vibration accelerations at four points were simultaneously measured under an operating condition, and a fast Fourier transform (FFT) analysis was performed (Ono Sokki, DS2104 [8]).

The power spectrum of the vibration acceleration was averaged for one second because the power spectrum was unsteady. A 1-kHz high-pass filter and a 10-kHz low-pass filter were applied to remove the vibration components caused by the motor, and those in the resonance frequency range, respectively. The averaging time of one second was long enough compared with 0.001 second, which was the maximum period of the filtered vibration acceleration.

Table 1 shows four operating conditions (Cases 1 to 4) of the hydraulic test pumps, which were one centrifugal pump and two types of mixed-flow pumps. The rotating speed was changed in the centrifugal pump. Therefore, the peripheral velocity at the impeller eye, U_e, was changed in Cases 1 and 2. In all Cases, the net positive suction head (*NPSH*) was nearly equal to the required NPSH ($NPSH_R$) in part-load conditions.

2.2 Measurement of Plastic Deformation Volume of Aluminum Sheet

Figure 2 (a) shows the state of a dye on the impeller blade after pump operation. A cavitation erosion area was visualized as the area of the dye peeling due to the cavitation bubble collapse. In Fig. 2 (a), the round peeling area appeared near the tip and the trailing edge of the impeller blade.

In the erosion area, a pure aluminum sheet was attached with a double-coated adhesive tape, as shown in Fig. 2 (b). The dimensions of the aluminum sheet were 20 x 20 mm. After running the pump, we observed many tiny pits caused by the cavitation bubble collapse. The pits were plastic deformations on the aluminum sheet surface. The plastic deformation of the sheet surface increased as the operation time increased. The surface shape was replicated with a resin, and the surface shape of the resin replica was measured using a 3-D laser scanning system (Hitachi Technologies and Services, LS-100 [9]).

This procedure (Fukaya [5], Udo [6]) was conducted for each test pump, and the time-variation of the plastic deformation volume of the aluminum sheet was obtained.

3. Results and Discussion

3.1 Scattered Vibration Acceleration depending on Sensor Position

Figure 3 shows the vibration accelerations measured at the four points on the centrifugal pump in Fig. 1. The subscript *m* of the vibration accelerations indicates the sensor number. In Fig. 3, α_m was nondimensionalized by α_1. The measured vibration acceleration on the suction pipe wall (No. 2) was larger than that on the upstream suction pipe wall (No. 3). The vibration acceleration depended on the distance between the bubble collapse location and the sensor. The measured vibration acceleration on the suction pipe wall (No. 2) was larger than that on the flange of the suction pipe (No. 1). This was because the distance between the bubble collapse location and the sensor was shorter for the sensor No. 2, and the suction pipe wall was thinner and had less stiffness compared with the flange of the suction pipe.

The vibration accelerations were varied, and the maximum vibration acceleration ratio, α_m / α_1, reached about 4 in this measurement. In the single-point vibration acceleration method (TSJ Guideline 2003 [4]), the cavitation intensity is estimated based on the vibration acceleration measured at one point without evaluating the pressure propagation path between the bubble collapse location and the sensor. Therefore, the varied vibration accelerations, as shown in Fig. 3, indicated varied cavitation intensities.

3.2 Multi-Point Vibration Acceleration Method

To accurately analyze the vibration accelerations, we theoretically defined a ‘pressure propagation coefficient.’ The pressure propagation coefficient is a new parameter that theoretically formulated the aforementioned damping rate, transmittance, and energy conversion along assumed pressure propagation paths.

In our method, we assumed that the bubble collapse pressure was generated at the mid-point of the impeller on the leading edge. The pressure propagation path between the bubble collapse point and the sensor was assumed to be one-dimensional as shown in Fig. 1. We assumed two representative paths, i.e.,

(A) path A along the pressure wave that propagated mainly in water and

(B) path B along the pressure wave that propagated mainly in solids.

When we lined the paths A and B, we determined the following rules to ensure that the paths were consistently constructed in different types of pumps.

(1) The straight lines that were parallel or vertical to the rotational axis of the impeller were given priority.

(2) Meanwhile, we selected the shortest distance between the assumed bubble collapse point and the sensor to estimate the pressure with minimum damping: (e.g. a path A shown as blue dotted line in Fig. 1 was not selected for the sensor No. 3.)

(3) In this procedure, the path in the solid between the water and the sensor was intended to be vertical with the solid surface where the sensor was attached.

(4) The path between the water and the sensor was also intended to avoid crossing the contact surfaces between the pipes, or between the pipe and the casing.

The bubble collapse pressure, p_c, generated at the bubble collapse point was assumed to propagate as a plane pressure wave with an initial amplitude of p_c and a frequency, f, of 5 kHz. Here, 5 kHz was adopted as a representative frequency in the filtered range of 1 to10 kHz. When the pressure wave propagated with a sound velocity, C, in a material that has a path length, L, the cycle number included in the path length was $L_i f_i / C_i$, where i was the material number (i = 1,2,…,n). The amplitude of the pressure

wave was damped to be $\exp\left(-\frac{L_i f}{C_i}\delta_i\right)$ after the propagation of the path length, where δ_i is the damping coefficient of pressure wave in the material. When the pressure wave was transmitted from a surface between different materials, the pressure amplitude was varied to $\tau_{pi} = \frac{2Z_{i+1}}{Z_i + Z_{i+1}}$, where $Z_i = \rho_i C_i$ is the acoustic impedance. Therefore, when the pressure wave propagated in different materials and reached the sensor, the amplitude of the pressure wave was described as

$$p_c \cdot \exp\left(-\frac{L_1 f}{C_1}\delta_1\right) \cdot \tau_{p1} \cdot \exp\left(-\frac{L_2 f}{C_2}\delta_2\right) \cdot \tau_{p2} \cdot \exp\left(-\frac{L_3 f}{C_3}\delta_3\right) \cdots\cdots \tau_{pn-1} \cdot \exp\left(-\frac{L_n f}{C_n}\delta_n\right) = p_c \prod_{i=1}^{n} \exp\left(-\frac{L_i f}{C_i}\delta_i\right) \cdot \prod_{i=1}^{n-1} \frac{2Z_{i+1}}{Z_i + Z_{i+1}} \quad . \tag{1}$$

The maximum amplitude of the pressure wave was expressed as the following equation with the plural paths taken into consideration.

$$\sum_{j=1}^{l} p_c \prod_{i=1}^{n} \exp\left(-\frac{L_i f}{C_i}\delta_i\right) \cdot \prod_{i=1}^{n-1} \frac{2Z_{i+1}}{Z_i + Z_{i+1}} = p_c \sum_{j=1}^{l} \left(\prod_{i=1}^{n} \exp\left(-\frac{L_i f}{C_i}\delta_i\right) \cdot \prod_{i=1}^{n-1} \frac{2Z_{i+1}}{Z_i + Z_{i+1}} \right) \tag{2}$$

where j is the path number, and the l is the total number of the paths. When the paths in Fig. 1 were assumed, j = 1 and j = 2 corresponded to paths A and B, respectively, and l = 2.

Because the pressure wave was damped very little in the solid part of the test pumps, the solid part, on which the sensor was attached, was vibrated by the pressure, $\rho_m L_m \alpha_m$. In this equation, ρ_m is the density of the solid part, L_m is the path length between the water and the sensor, α_m is the measured vibration acceleration, and the subscript m indicates the sensor number. The pressure was equivalent to the pressure expressed by eq. (2). Then,

$$\rho_m L_m \alpha_m = p_c \sum_{j=1}^{l} \left(\prod_{i=1}^{n} \exp\left(-\frac{L_i f}{C_i}\delta_i\right) \cdot \prod_{i=1}^{n-1} \frac{2Z_{i+1}}{Z_i + Z_{i+1}} \right) \quad , \text{ i.e.,} \tag{3}$$

$$\alpha_m = p_c \frac{\sum_{j=1}^{l} \left(\prod_{i=1}^{n} \exp\left(-\frac{L_i f}{C_i}\delta_i\right) \cdot \prod_{i=1}^{n-1} \frac{2Z_{i+1}}{Z_i + Z_{i+1}} \right)}{\rho_m L_m} \quad . \tag{4}$$

The 'pressure propagation coefficient,' R_{pm}, was defined as

$$R_{pm} \equiv \frac{\sum_{j=1}^{l} \left(\prod_{i=1}^{n} \exp\left(-\frac{L_i f}{C_i}\delta_i\right) \cdot \prod_{i=1}^{n-1} \frac{2Z_{i+1}}{Z_i + Z_{i+1}} \right)}{\rho_m L_m} \quad . \tag{5}$$

Equation (4) was simplified to become eq. (6).

$$\alpha_m = p_c R_{pm} \tag{6}$$

Equations (5) and (6) indicate that the pressure propagation coefficient, R_p, was a theoretical correlation coefficient between the vibration acceleration and the bubble collapse pressure.

When the bubble collapse pressure, p_c, was assumed to be constant under a certain operation condition of the pump, the vibration acceleration, α_m, was theoretically proportional to R_{pm}. We considered the overlap of the vibration acceleration, β, which was caused by the motor and the fluid phenomena with the exception of cavitation. The coefficient β is a constant that is different in each pump. Then, eq. (6) was improved:

$$\alpha_m = p_c R_{pm} + \beta \tag{7}$$

Figure 4 shows the vibration accelerations measured in the test pumps, which were correlated with the pressure propagation coefficient. The vibration acceleration, α_m, was nondimensionalized by α_1 in each pump. The vibration accelerations increased proportionally as the pressure propagation coefficient increased. The lines in Fig. 4 show the approximate straight lines that were calculated with the least squares method. The gradient of the straight line corresponded to the bubble collapse pressure based on eq. (7). The cavitation intensity, I, was predicted by the following equation (Soyama [2]),

$$I = \frac{p_c^{\,2}}{2\rho_w c_w} \quad , \tag{8}$$

where ρ_w is the water density, and c_w is the sound velocity in water.

The approximate straight line can be obtained based on at least two vibration acceleration data. However, the prediction accuracy of the gradient of the straight line, that is the bubble collapse pressure, depends on the number of the vibration acceleration data. In the present study, four vibration acceleration data were analyzed in each pump to improve the prediction accuracy of the bubble collapse pressure. For further improvement of the prediction accuracy, the number of sensor should be increased considering that the pressure propagation coefficients are sufficiently different from each other.

3.3 Examination of Prediction Accuracy of Cavitation Intensity

Figure 5 shows the time-variation of the plastic deformation volume of the aluminum sheet in the cavitation erosion area. The plastic deformation volume, ΔV, was measured in the region of 5 x 5 mm near the center of the 20 x 20 mm aluminum sheet. The plastic deformation volume was the increment from the initial state. ΔV_0 was the standard value of ΔV, which was obtained after pump operation of 900 seconds in Case 1. In Fig. 5, ΔV in all pumps was nondimensionalized by ΔV_0.

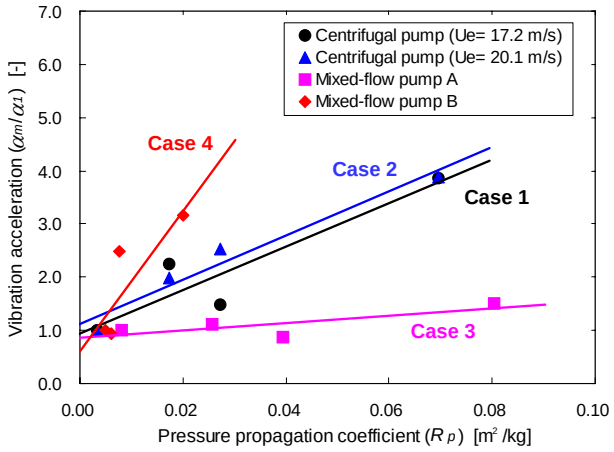

Fig. 4 Relationship between pressure propagation coefficient and measured vibration acceleration

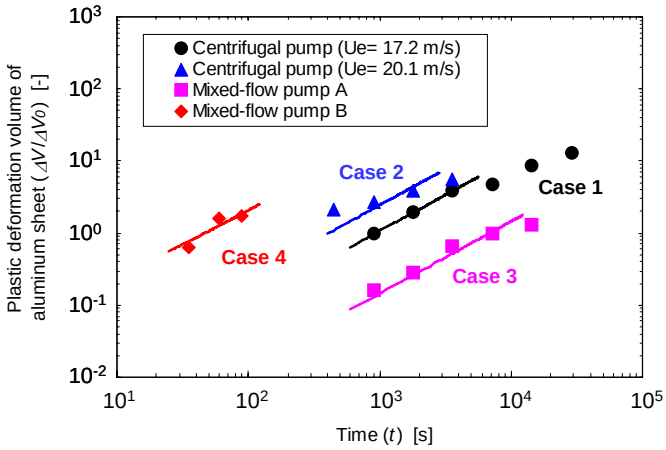

Fig. 5 Time-variation of plastic deformation volume of aluminum sheet measured with laser 3-D measurement system

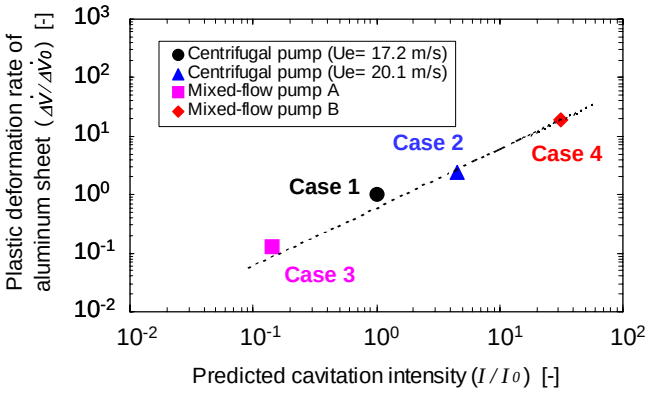

(a) Multi-point vibration acceleration method

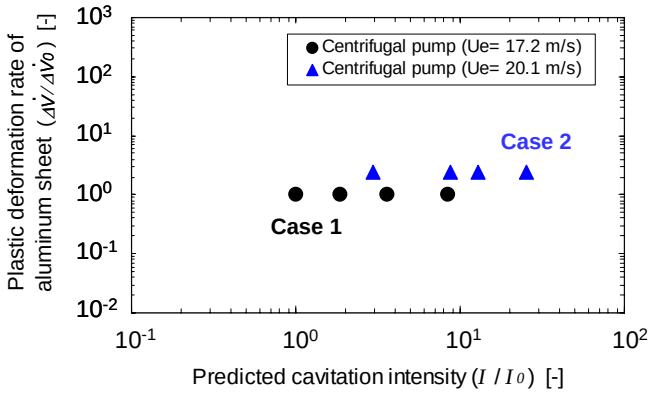

(b) Conventional vibration acceleration method

Fig. 6 Relationship between predicted cavitation intensity and plastic deformation rate of aluminum sheet

The rate of increase in the plastic deformation volume was nearly constant within a certain time after the pump operation was started. The time range at the constant rate was different in Cases 1 and 4. After the time range at the constant rate, the rate of increase tended to fall gradually over time. The approximate straight lines through the origin were calculated by the least squares method. The plastic deformation rate was defined as the gradient of the approximate straight line within the time range of the constant increase rate.

In a previous study, the correlation between the plastic deformation rate of the aluminum sheet and the cavitation intensity was analyzed using a cavitating jet apparatus (Fukaya [5], Udo [6]). The data was obtained with the same aluminum sheet in Fig. 2 (b) and the piezoelectric film sensor (Soyama [2]). The plastic deformation rate was proportional to the cavitation intensity. Therefore, the plastic deformation rate measured in the test pumps was regarded as the criterion of the cavitation intensity in the present study.

Figure 6 (a) shows the correlation between the estimated cavitation intensity by using our method and the plastic deformation rate as shown in Fig. 5. The cavitation intensity was obtained from the results in Fig. 4 based on eqs. (7) and (8). The cavitation intensity and the plastic deformation rate were nondimensionalized by those in Case 1. The plastic deformation rate increased proportionally as the estimated cavitation intensity increased.

In the single-point vibration acceleration method (TSJ Guideline 2003 [4]), the cavitation intensity was predicted by the following equation with the vibration acceleration, G, which was measured on the casing,

$$I = a\left(\frac{G}{n^2 D_2}\right)^b \left(\frac{P_w}{D_2{}^2}\right) \quad , \tag{9}$$

where n and D_2 are the rotating speed and the outer diameter of the impeller, respectively, P_w is the water power of the pump at a maximum efficiency point, and a and b are experimental constants, which depend on the type, structure, and material of the pumps. The TSJ Guideline 2003 [4] showed $a = 2 \times 10^{-7}$ and $b = 1.58$, both of which were estimated in a centrifugal pump having a single-suction volute.

The test pumps in the present study were different from the pump in the TSJ Guideline 2003 [4] concerning the type, structure, and material. Therefore, the aforementioned values of a and b were not available. However, we attempted to apply eq. (9) to the vibration accelerations measured in Cases 1 and 2, because the centrifugal pump had a single-suction volute.

Figure 6 (b) shows the predicted cavitation intensity based on eq. (9). The cavitation intensities had a difference of about one order at maximum, e.g., I/I_0 was from 1 to 10 in Case 1. This result showed that the experimental constants, a and b, needed to be estimated for each sensor position.

The comparison between our method and the single-point vibration acceleration method (TSJ Guideline 2003 [4]) showed that the prediction accuracy of the cavitation intensity was higher in our method without the experimental constants.

3.4 Cavitation Intensity Map

Figure 7 shows the cavitation intensity map of the centrifugal pump including Case 1. We obtained the map using our method and varying the flow rate and the net positive suction head (*NPSH*). The *NPSH* was nondimensionalized by $NPSH_R$ at a flow rate of 100%. The cavitation intensity was divided to be dimensionless by the cavitation intensity, I_1, under the condition of $NPSH_R$ at a flow rate of 100%. There were several measurement points of the cavitation intensity at each flow rate of 0, 20, 40, 60, 80, 100, 120, 140 and 155%. The cavitation intensity in the region outside the measurement points was interpolated with those on the measurement points.

When the flow rate was less than 40% or at 155%, high-cavitation-intensity regions were formed; however, the region was far from the normal operation condition. The local high-cavitation-intensity region also appeared around the condition of Q = 80% and dimensionless *NPSH* = 2.3. We found that we had to avoid this condition during normal operation. The map is useful for avoiding the operating conditions having high risk of cavitation erosion.

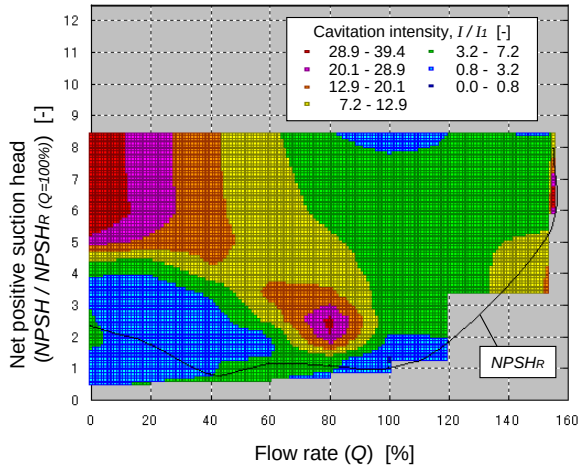

Fig. 7 Cavitation intensity map based on multi-point vibration acceleration method

4. Conclusions

We developed a 'multi-point vibration acceleration method' for predicting the cavitation intensity in pumps accurately and practically. This method estimates the cavitation intensity without experimental constants as proposed in a conventional method by analyzing the vibration accelerations measured at multi-points with the 'pressure propagation coefficient'. The pressure propagation coefficient theoretically formulates the factors, which cause the dependency of the vibration acceleration on the sensor position. The prediction accuracy of cavitation intensity was improved based on a statistical analysis of the multi-point vibration accelerations. We verified the predicted cavitation intensity with the plastic deformation rate of an aluminum sheet attached in the bubble collapse area of the impeller blade. The prediction accuracy of the cavitation intensity based on our method was improved over that of the conventional method based on the vibration acceleration measured at one point on the pump casing. The cavitation intensity map was obtained by conducting the multi-point vibration acceleration method. The map was useful for accurately searching for the operating conditions having high risk of cavitation erosion.

Nomenclature

C	Sound velocity [m/s]	Q	Flow rate [m^3/min]
f	Frequency of pressure wave [Hz]	R_p	Pressure propagation coefficient [m^2/kg]
D_2	Outer diameter of impeller [m]	ΔV	Plastic deformation volume [mm^3]
G	Acceleration vibration [m/s^2]	$\dot{\Delta V}$	Plastic deformation rate [mm^3/s]
I	Cavitation intensity [W/m^2]	Z	Acoustic impedance [kg/m^2 s]

L	Path length [m]	α	Acceleration vibration [m/s^2]
n	Rotating speed of impeller [s^{-1}]	β	Acceleration vibration caused by phenomena except cavitation [m/s^2]
$NPSH$	Net positive suction head [m]		
$NPSH_R$	Required net positive suction head [m]	δ	Damping coefficient of pressure wave [-]
p_c	Bubble collapse pressure [Pa]	ρ	Density [kg/m^3]

References

[1] Konno, A., et al., 2001, "On the collapsing behavior of cavitation bubble clusters," Proc. of Fourth Int. Symposium on Cavitation (CAV2001), Pasadena, CA/USA, session A8.003.

[2] Soyama, H. and Kumano, H., 2002, "The Fundamental Threshold Level - a New Parameter for Predicting Cavitation Erosion Resistance", J. of Testing and Evaluation, ASTM Int., pp. 421-431.

[3] Maekawa, M., et. al., 2003, "Study of Cavitation on Hydraulic Turbine Runners," Proc. of 5th Int. Symposium on Cavitation (CAV2003), Osaka, Japan, Cav03-OS-6-015.

[4] Turbomachinery Society of Japan, 2003, "TSJ Guideline; Guideline for Prediction and Evaluation of Cavitation Erosion in Pumps (in Japanese)," TSJ G 001:2003. (in Japanese)

[5] Fukaya, M., et. al., 2006, "Experimental Prediction Method of Cavitation Erosion in Pumps by Using Aluminum Sheet," Proc. of 6th Int. Symposium on Cavitation (CAV2006), Wageningen, The Netherlands, 104.

[6] Udo, R., et. al., 2006, "Measurement of Cavitation Intensity in Pumps by Using Aluminum Sheet," Proc. of 6th Int. Symposium on Cavitation (CAV2006), Wageningen, The Netherlands, 122.

[7] Ono Sokki, http://www.onosokki.co.jp/HP-WK/products/keisoku/soundvib/np2000_series.html.

[8] Ono Sokki, http://www.onosokki.co.jp/HP-WK/products/keisoku/data/ds2000.html.

[9] Hitachi Technologies and Services, Ltd., http://www.hitachi-ts.co.jp/business/engineering/testing/laser3d/index.html.